Scientia Iranica A (2014) 21(3), 534–547

Sharif University of Technology
Scientia Iranica
Transactions A: Civil Engineering
www.scientiairanica.com

A novel force-based approach for designing armor blocks of high-crested breakwaters

A. Pak* **and M. Sarfaraz**

Department of Civil Engineering, Sharif University of Technology, Tehran, P.O. Box 11155-9313, Iran.

Received 15 April 2013; received in revised form 5 September 2013; accepted 24 September 2013

KEYWORDS
Wave forces;
Breakwaters;
Armor units stability;
Numerical modeling.

Abstract. Rubble-mound breakwaters are common marine structures that provide a safe area for human coastal activities. The stability of these structures against sea-waves requires their seaward slope to be protected by an armor layer consisting of natural rock or concrete units. To provide a safe breakwater, it is reasonable to establish a relation between the exerted wave loads and the stability of the armor units. However, up to now, the empirical design equations, derived from model tests, relate wave parameters to armor weight, and keeps the effect of wave loads in a black box. In this paper, a new approach, based on numerically-derived wave loads on the armor, is presented to evaluate the stability of these protective units. Results indicate that by increasing wave height, the weight of the armor units does not necessarily increase. Wave breaking type strongly influences the applied loads and stability of the armor units. New dimensionless numbers are introduced to provide relationships between wave parameters and stability indices of breakwater armor units at different locations. This approach clarifies the ambiguities of the design process caused by the complex flow field, especially the wave breaking type near the breakwater.

1. Introduction

Breakwaters play an important role in providing a calm and safe area in coastal waters. The most widely used breakwater type is the rubble-mound, whose surface is protected by rock or concrete units. The armor units should remain motionless or have allowable movement only during stormy conditions [1].

Currently, determining the stable weight of breakwater armor units is largely reliant on using some empirical formulae, such as Hudson [2] and van der Meer [3], based on calibration of laboratory wave flume results. These formulae are proposed mostly for rock stones, rather than concrete blocks [1].

The Hudson formula, presented in 1959, is given by Eq. (1) [2]:

$$\frac{H}{\Delta D_{n50}} = (K_D \cot\alpha)^{\frac{1}{3}}, \tag{1}$$

where H, Δ, D_{n50}, K_D and α are wave height, relative mass density, nominal diameter, stability coefficient and slope angle, respectively. The Hudson formula is based solely on wave height and does not consider the effects of wave period, wave length, and breaking type [3].

van der Meer, in 1990 [3], presented formulae in which the effects of the wave period and its length are included. It should be pointed out that the formulae are presented for plunging (Eq. (2)) and surging breaking (Eq. (3)) types, but the collapsing type is not directly addressed:

$$\frac{H\sqrt{\varepsilon}}{\Delta D_{n50}} = 6.2P^{0.18}\left(\frac{S_d}{\sqrt{N}}\right)^{0.2}, \tag{2}$$

$$\frac{H}{\Delta D_{n50}} = 1.0P^{-0.13}\left(\frac{S_d}{\sqrt{N}}\right)^{0.2}\varepsilon^P\sqrt{\cot\alpha}\,, \tag{3}$$

*. *Corresponding author. Tel.: +98 21 66164225*
E-mail addresses: pak@sharif.edu (A. Pak); sarfaraz@alum.sharif.edu (M. Sarfaraz)

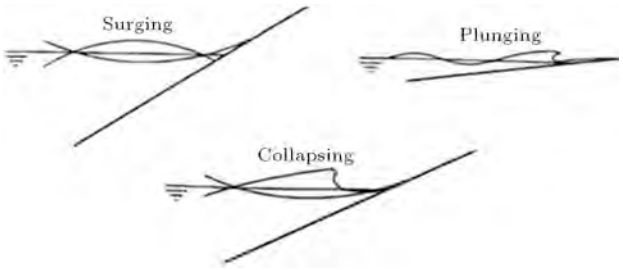

Figure 1. Wave breaking type configuration [4].

where ε is the surf similarity parameter (Iribarren number), $\varepsilon = \frac{\tan\alpha}{\sqrt{2\pi H/L}}$, L is the wave length, P is the permeability coefficient and, finally, S_d is the damage level. For estimating values of P and S, reader is referred to [3]. The breaking type forms are shown in Figure 1.

It is reasonable to assume that for a more rational and economical design, a relation between the exerted wave loads and stability of the armor units must be established. However, up to now, the common design methodology simply relates the accessible wave parameters (e.g. wave height and period) directly to the armor weight and keeps the effect of wave loading in a black box. This approach can be observed in the well-known Hudson and van der Meer formulae. Few studies about the wave forces acting on armor units have been conducted so far, mostly by physical tests on submerged breakwaters.

Sigurdsson, in 1962 [5], measured wave forces acting on a group of plastic spheres, idealized for armor, on a submerged breakwater. It was concluded that the magnitude of forces on the armor significantly increases when experiencing a breaking wave.

Apelt and Piorewicz, in 1987 [6], conducted tests in a laboratory to measure the breaking wave forces on a pile on the beach. They showed that there exists no monotonic relation between the force magnitudes and wave parameters, which is related to the complex mechanism of wave breaking.

Mizutani et al., in 1993 [7], measured wave forces on sphere armors of the same diameter located on a submerged breakwater. Results showed that a complex relationship exists between the exerted force to the armor and wave parameters.

Oumeraci et al., in 1993 [8], conducted experimental tests to analyze wave breaking force on a vertical sea-wall. The analysis proved that the force does not necessarily increase with the rise of wave height. In fact, the type of wave breaking was found to affect the relation between the force magnitudes and wave parameters.

Pramono, in 1997 [9], analyzed the stability of the armor layers by measuring wave forces acting on a single armor unit located on a submerged breakwater. Two instability numbers were introduced for sliding and overturning failure modes of the armor. The results did not yield well-behaved curves. An important result of the research was that increasing the wave height did not raise the instability numbers monotonically.

The physical modeling of wave-structure interactions do not usually follow similitude laws for all significant forces, which may influence prediction regarding the behavior of a prototype [10]. Due to this kind of limitation, there is a tendency for researchers to seek for near-prototype scale physical tests of about 1:5 or less. However, only few such massive and costly laboratory apparatuses exist. The consequential costs of moving towards larger physical tests, because of uncertainties posed by small-scale flume tests, are widely recognized by coastal engineers [11].

Since numerical modeling does not undergo scale problems [12,13], it can be used, along with physical tests, to increase our understanding about the stability of armor layers in breakwaters.

Several numerical studies have been performed in coastal engineering, such as modeling wave run-up, wave breaking [13], and modeling flow field around the breakwaters [12,14,15]. Besides, some attempts have been made to numerically calculate the exerted wave loads on coastal structures. Guanche et al., in 2009 [16], used the numerical model, COBRAS-UC, to address the wave loads for a vertical caisson on a rubble-mound structure. In their research, the exerted wave load was calculated by integrating the pressure field around the structure, neglecting the effect of shear stress, which can lead to inaccuracy of results.

In this paper, it is intended to use numerical modeling for evaluating the stability of armor units of high-crested breakwaters, based on numerically-derived wave loads and the equilibrium concept instead of empirical formulae, which provides a solid ground for designing breakwaters. A two-dimensional numerical model is used to calculate wave-induced loads on the armor units located on a high-crested breakwater. Three failure modes for the armor were introduced and the corresponding instability numbers were calculated based on the derived forces. The proposed approach to the design of breakwaters can be developed later to address the armor unit stability problem when the interaction of neighboring blocks are considered in the analysis.

2. Description of the numerical model

The principle equations used in this study are continuity and Navier-Stokes (N-S) equations. To contain the turbulence effects, Large Eddy Simulation (LES) was chosen, amongst other turbulence models, due to its more accurate results in the current problem [17]. The LES is concerned with finding suitable approximations

to account for the influence of the small-scale eddies. This is done by incorporating a sub-grid scale model, and by directly computing the large energy-carrying eddies [18]. The continuity and N-S equations can be written, respectively, as:

$$\frac{\partial \bar{u}_i}{\partial x_i} = 0, \quad i = 1, 2, 3, \tag{4}$$

$$\frac{\partial \bar{u}_i}{\partial t} + \frac{\partial}{\partial x_j}\bar{u}_i\bar{u}_j = -\frac{\partial \bar{P}}{\partial x_i} + \frac{\partial}{\partial x_j}[\nu\left(\frac{\partial \bar{u}_i}{\partial x_j} + \frac{\partial \bar{u}_j}{\partial x_i}\right) - \tau_{ij}] + \rho g_i, \quad i, j = 1, 2, 3\ , \tag{5}$$

where $\bar{u}_i$ is the velocity component in direction i, $\bar{P}$ is the corresponding pressure, g is the gravity acceleration, and τ_{ij} is the stress tensor describing the influence of small-scale eddies on larger (resolved) eddies. This is the only effect to be modeled by a sub-grid scale model, which is written as [19]:

$$\tau_{ij} - \frac{1}{3}\delta_{ij}\tau_{kk} = -2\upsilon_T \bar{S}_{ij}, \tag{6}$$

$$\bar{S}_{ij} = \frac{1}{2}\left(\frac{\partial \bar{u}_i}{\partial x_j} + \frac{\partial \bar{u}_j}{\partial x_i}\right), \tag{7}$$

where δ_{ij} is the Kronecker delta, $\bar{S}_{ij}$ is the strain rate tensor for the resolved scale, and υ_T is the eddy viscosity, which was calculated in this case by the Smagorinsky model.

The Volume Of Fluid (VOF) technique was applied to treat the free surface by a step function, F. This technique has been applied successfully to resolve details of free surface dynamics and breaking type (e.g. [12,13]). The transport equation for VOF is governed by [20]:

$$\frac{\partial F}{\partial t} + \bar{u}_i\frac{\partial F}{\partial x_i} = 0. \tag{8}$$

Linear wave theory was employed to define the flow parameters at the incoming wave boundary. Horizontal and vertical velocity components and pressure are computed by Eqs. (9)-(11), respectively [21]:

$$u = \frac{gHT}{2L}\frac{\cosh\left(\frac{2\pi(z+d)}{L}\right)}{\cosh\left(\frac{2\pi d}{L}\right)}\cos\left(\frac{2\pi t}{T}\right), \tag{9}$$

$$\nu = \frac{-gHT}{2L}\frac{\sinh\left(\frac{2\pi(z+d)}{L}\right)}{\cosh\left(\frac{2\pi d}{L}\right)}\sin\left(\frac{2\pi t}{T}\right), \tag{10}$$

$$p = \frac{\rho g H\cosh\left(\frac{2\pi(z+d)}{L}\right)}{2\cosh\left(\frac{2\pi d}{L}\right)}\cos\left(\frac{2\pi t}{T}\right) - \rho g z, \tag{11}$$

where H, T and L are the height, period and length of the wave, respectively; z is the vertical distance from the Still Water Level (S.W.L.) and, finally, d is the S.W.L. depth.

Hydraulic forces acting on the body of the armor units are determined by [22]:

$$\vec{F} = \int\int pndA + \int\int \tau dA, \tag{12}$$

where dA is the solid surface area and n is the unit vector normal to area, dA.

In this research, FLOW-3D was employed to solve the equations and obtain the above-mentioned flow field parameters induced by the incoming regular waves in a 2D space, by utilizing finite difference/finite volume approximation [23]. The code was validated against some experimental data and empirical equations, showing that the physical and the numerical results are in good agreement [17].

For evaluating wave loads acting on armor units, four different locations are selected, namely: toe of the breakwater (L1), still water level (L2), wave run-up elevation (L3) and wave run-down elevation (L4), as depicted in Figure 2. The breakwater is assumed to be impermeable and high-crested with a uniform face slope. The armor units are assumed individual blocks, cubic in shape, and stationary. It should be noted that other types of armor block can also be considered, but, since this is the first attempt to determine wave-induced forces on armor units and evaluate breakwater stability employing a force-based approach, it was decided that the simple cube units be analyzed at the first stage. Other parameters used in the numerical analysis are wave height (H), wave period (T), still water depth (D), breakwater face slope (S) and armor block length (A) whose variations are demonstrated in Table 1.

The distance between the incoming wave boundary and toe of the breakwater is 460 m, almost equal to 5 times the longest wave length.

It should be noted that all combinations of the parameters shown in Table 1 are not analyzed. As shown later, more variety of combinations are allocated to L2

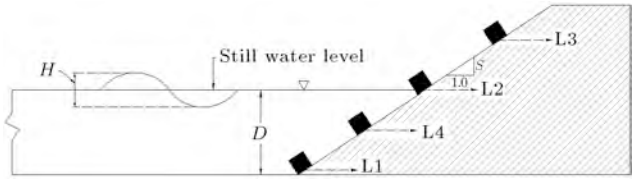

Figure 2. Definition of the structural parameters.

Table 1. Main parameters employed in the numerical study.

Armor location	A (m)	S	D (m)	T (s)	H (m)
Toe (L1)	1.0	1V:1.5H	10	5	2
Still water level (L2)	1.5	1V:2.0H	15	7	3
Run-up elevation (L3)	2.0	1V:2.5H	–	10	4
Run-down elevation (L4)	–	–	–	–	5
–	–	–	–	–	6

Table 2. Combinations of the parameters for each armor location.

Parameters	L1	L2			L3		L4
		Subset 1	Subset 2	Subset 3	Subset 1	Subset 2	
H (m)	4, 5, 6	4, 5, 6	2, 3	2	4, 5, 6	4, 5, 6	4, 5, 6
T (s)	5, 7, 10	5, 7, 10	10	7	5, 7, 10	5, 7, 10	5, 7, 10
D (m)	10, 15	10, 15	10, 15	15	10, 15	10	10, 15
S (1V:H)	1.5	1.5, 2, 2.5	2.5	2.5	1.5	1.5	1.5
A (m)	1	1, 1.5, 2	1, 1.5, 2	1, 1.5, 2	1	1.5	1, 1.5, 2
# combination	18	162	12	3	18	9	54

and L4, due to be the more critical locations. Combinations of the parameters for analysis of armor unit stability at different locations are shown in Table 2.

In this paper, a new approach for analyzing the stability of armor units is employed. The stability of slopes is primarily a geomechanical problem, in which the height and inclination angle of the slope and unit weight of the soil/rock play major roles. In the case of mound breakwaters, the wave height and depth of water play important roles as well. If the conventional limit equilibrium approach for stability analysis is considered, then, "failure modes" should first be identified, and for evaluating the possibility of failure for each mode, a relevant factor of safety should be defined. For an armor block resting on the seaward face of a mound breakwater, three instability modes of uplifting (tendency of the armor to move perpendicular to breakwater slope), sliding (tendency of the armor to move parallel to breakwater slope, downward or upward) and overturning (tendency of the armor to rotate on its two edges, downward or upward) can be imagined. The corresponding factors of safety for each failure mode, denoted by U.I.N (Uplift Instability Number), S.I.N. (Sliding Instability Number) and O.I.N. (Overturning Instability Number), can be determined as follows:

$$\text{U.I.N} = \frac{F_{\text{instability}}}{F_{\text{resistance}}} = \frac{F_n}{W\cos\alpha}, \quad \text{failure} : \text{U.I.N} > 1, \tag{13}$$

$$\text{S.I.N.} = \frac{\Sigma F_{\text{instability}}}{F_{\text{resistance}}} = \frac{F_p - W\sin\alpha}{F_f},$$

$$\text{failure} : |\text{S.I.N.}| > 1, \tag{14}$$

$$\text{O.I.N.}_a = \frac{\Sigma M_{\text{instability}}}{\Sigma M_{\text{resistance}}} = \frac{F_n\frac{A}{2} + W(\sin\alpha)\frac{A}{2}}{M_y + F_p\frac{A}{2} + W(\cos\alpha)\frac{A}{2}}, \tag{15}$$

$$\text{O.I.N.}_b = \frac{\Sigma M_{\text{instability}}}{\Sigma M_{\text{resistance}}} = \frac{F_n\frac{A}{2} + F_p\frac{A}{2} + M_y}{W\cos\alpha\left(\frac{A}{2}\right) + W\sin\alpha\left(\frac{A}{2}\right)}, \tag{16}$$

$$\text{O.I.N.} = \max\{\text{O.I.N.}_a, \text{O.I.N.}_b\},$$

$$\text{failure} : |\text{O.I.N.}| > 1\ , \tag{17}$$

where F_n, F_p and M_y are components of the wave-induced forces and moment acting on the armor blocks, respectively, which are calculated by the software over time. F_f is the friction force between the armor unit and breakwater slope surface, and W is the armor weight (Figure 3). In the current research, analysis of the sliding and overturning instability modes are conducted, regardless of their direction; so, their absolute magnitudes are considered.

Friction coefficient and armor density are selected to be equal to 0.6 and 2300 kg/m^3, respectively [24]. The surface roughness of the breakwater face and the armor is assumed equal to 1.5 mm [25].

Maximum values of total force ($F_R = \sqrt{F_n^2 + F_p^2}$), |U.I.N|, |S.I.N.| and |O.I.N.|, are considered and discussed in this paper.

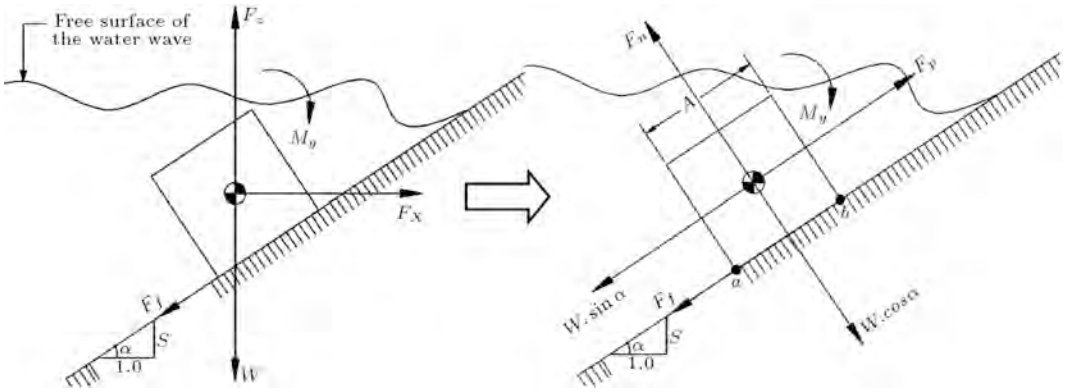

Figure 3. Definition of the forces used in calculating instability numbers.

Table 3. Mesh independency, $S = 1 : 1.5, T = 5$ s, $H = 6$ m, $D = 15$ m, $A = 1$ m, and location L2.

Mesh size (m)	Variation (%)			
	max.F_R	ave.F_R	max.$\lvert M_y \rvert$	ave.$\lvert M_y \rvert$
0.14	–	–	–	–
0.105	11.35	12.09	8.64	10.03
0.05	10.69	12.79	10.86	13.95
0.038	7.61	5.34	7.72	7.54
0.031	1.21	1.71	1.05	1.32
0.025	1.01	0.21	0.42	0.31

To select the appropriate mesh size and to ensure the mesh independency of the results, six element sizes were chosen, from 0.14 m to 0.025 m, to compare the maximum and average of total force (F_R) and moment ($|M_y|$) for the case of $S = 1 : 1.5$, $T = 5$ s, $H = 6$ m, $D = 15$ m, $A = 1$ m and location L2 (Table 3). As expected, by using smaller elements, more accurate results can be obtained. However, changes in the calculated values of F_R and $|M_y|$ become negligible (i.e. less than 2%) when the element size becomes less than 0.038 m. So, 0.038 m was selected for the size of the mesh. It is noted that the same procedure was repeated for other wave parameters and the same result was achieved.

3. Results and discussion

In this part, the magnitudes of the maximum wave-induced forces and moments, and instability numbers for different armor locations under wave action are presented by introducing some dimensionless numbers, which relate these magnitudes to the wave parameters.

3.1. Wave breaking type

For illustration, Figure 4 depicts wave breaking types captured by the numerical model for the slope of $S = 1.0 : 1.5$ and different values of Iribarren number. It is evident that by increasing ε, the breaking type changes from plunging to surging.

By inspection of the free surface profiles, Figure 5 can be drawn to show variation of the breaking type, for different values of ε and the breakwater face slope. It is demonstrated that for a certain ε value, by increasing the slope, the breaking type changes from surging to plunging.

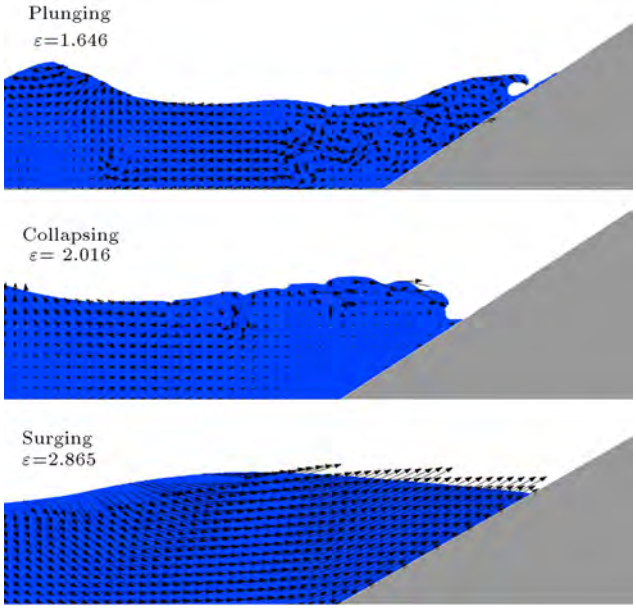

Figure 4. Wave breaking types, $S = 1.0 : 1.5$.

3.2. Total forces and moments

Surface wave profile running up the slope, for the case of $S = 1 : 1.5, T = 5$ s, $H = 6$ m, $D = 15$ m and

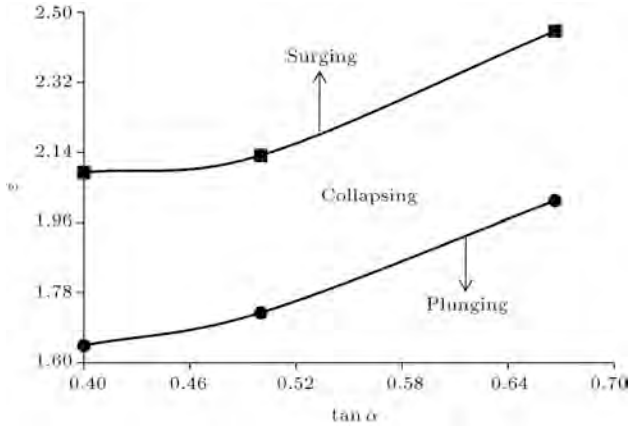

Figure 5. Wave breaking type classification.

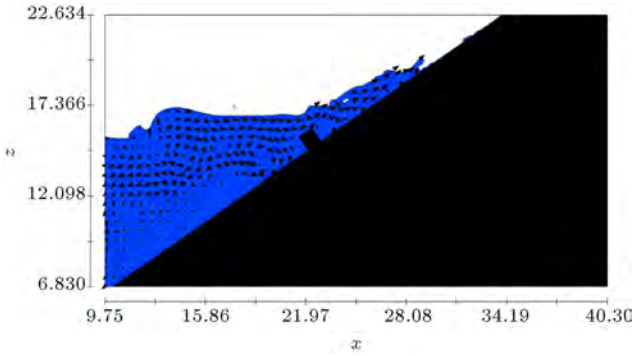

Figure 6. Surface wave profile around location L2, $S = 1.0 : 1.5$, $H = 6$ m, $T = 5$ s, $D = 10$ m and $A = 1$ m.

$A = 1$ m, near the location L2 (still water level), is presented in Figure 6. This figure shows a complex flow field near the armor unit, within the main part of the vortex field caused by the breaking wave.

Figure 7 represents variation of the maximum values of wave forces (F_R) with wave height for the case of $S = 1.0 : 1.5, D = 10$ m, different periods and armor lengths. The Iribarren number is also depicted on the right axis for examining the breaking type. It is shown, for the cases of $T = 5$ or 10 s, that an increase in wave height will lead to an increase in wave load, F_R, on the armor unit. However, for $T = 7$ s, the trend is inverse. The Iribarren number indicates that for the latter case, the breaking type is collapsing (Figure 5).

Similar figures for variation of F_R, with respect to wave height at $D = 15$ m, can be drawn. They all result in the exerted load, F_R, on the armor units having no monotonic relation with wave parameters.

To analyze the obtained results, employing dimensionless values that create well-behaved curves is required. Figure 8 illustrates variations of F_R in the form of the dimensionless number, $F_R^{0.2}\gamma_w^{0.2}/g^{0.2}\mu^{0.4}$($\gamma_w$ = density of water, g=gravity acceleration and μ=dynamic viscosity of water), versus Iribarren number for different breakwater slopes. Also, in this figure, wave breaking types are demonstrated.

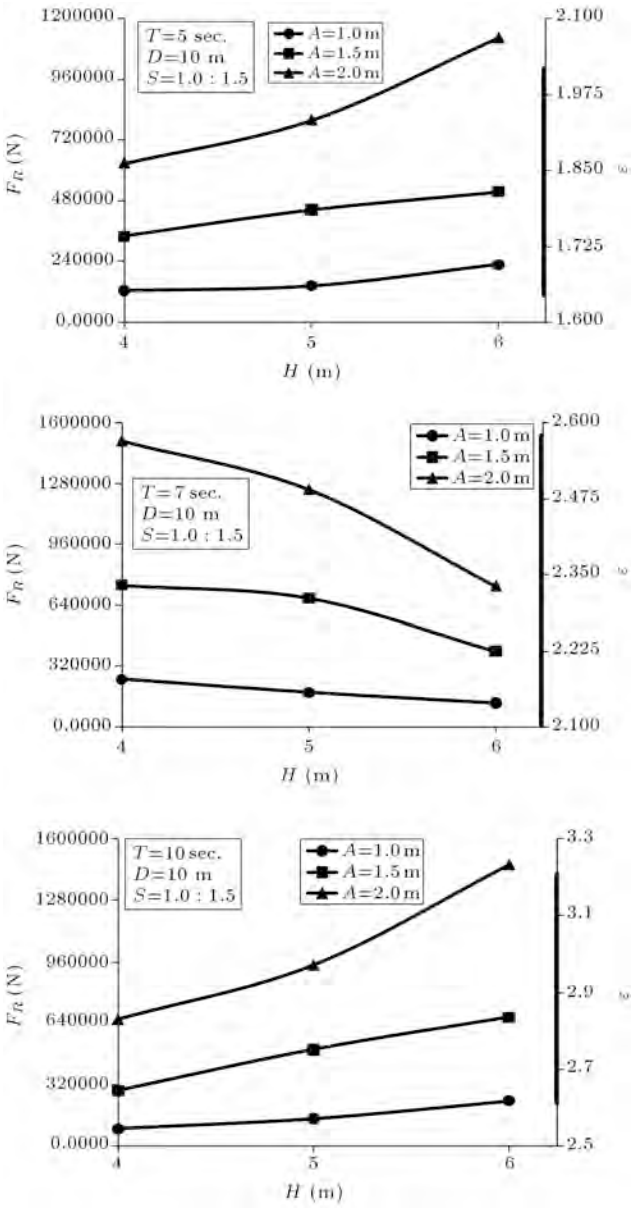

Figure 7. Variation of the maximum wave force with wave height for location L2, $S = 1 : 1.5$.

This figure points out that the relation between the applied forces on the armor and the wave parameters is not monotonic. The reason lies in the type of wave breaking mechanism. In surging and plunging types, by increasing the wave height or decreasing the wave period, the applied force increases, where this is contrary for the collapsing breaking type.

A similar trend is valid for the maximum moment applied to the armor ($|M_y|$) which is shown in Figure 9.

Figure 10 presents variation of the maximum wave forces and moments versus ε for location L4 (minimum wave run-down level). This figure shows a similar trend with case L2, in which a monotonic relation does not exist between the parameters in the small range of Iribarren number variation. But, in this location, the

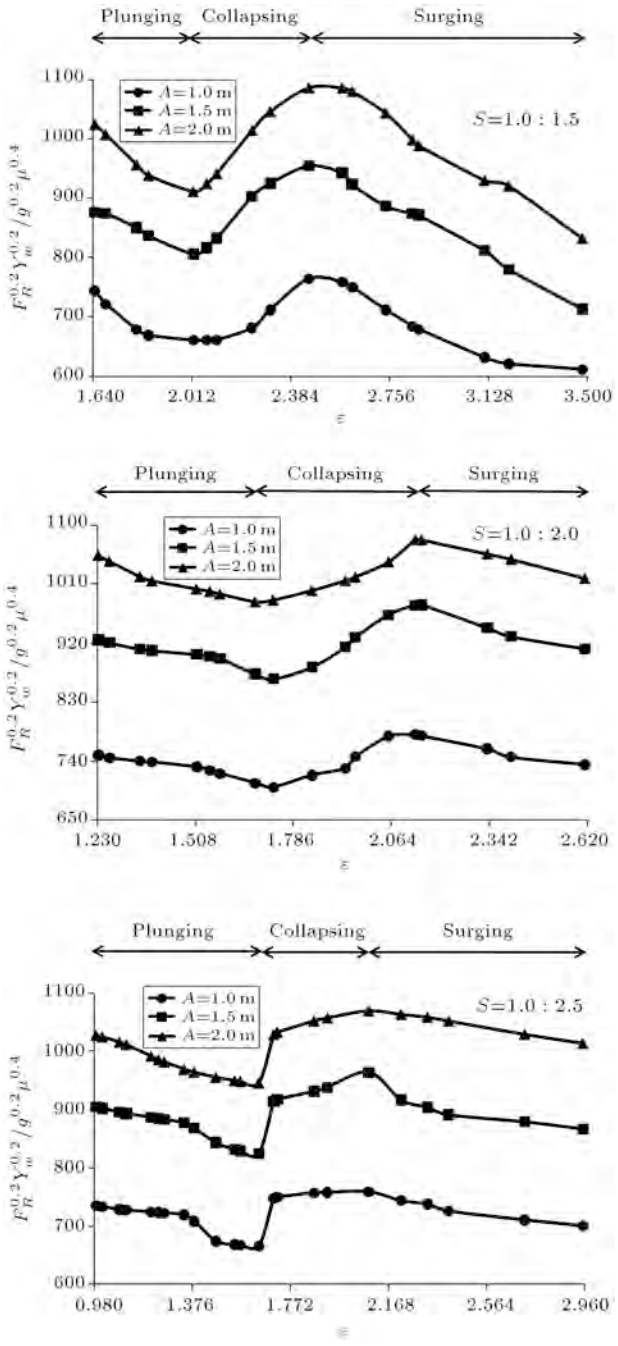

Figure 8. Variation of maximum wave force for location L2 versus wave parameters.

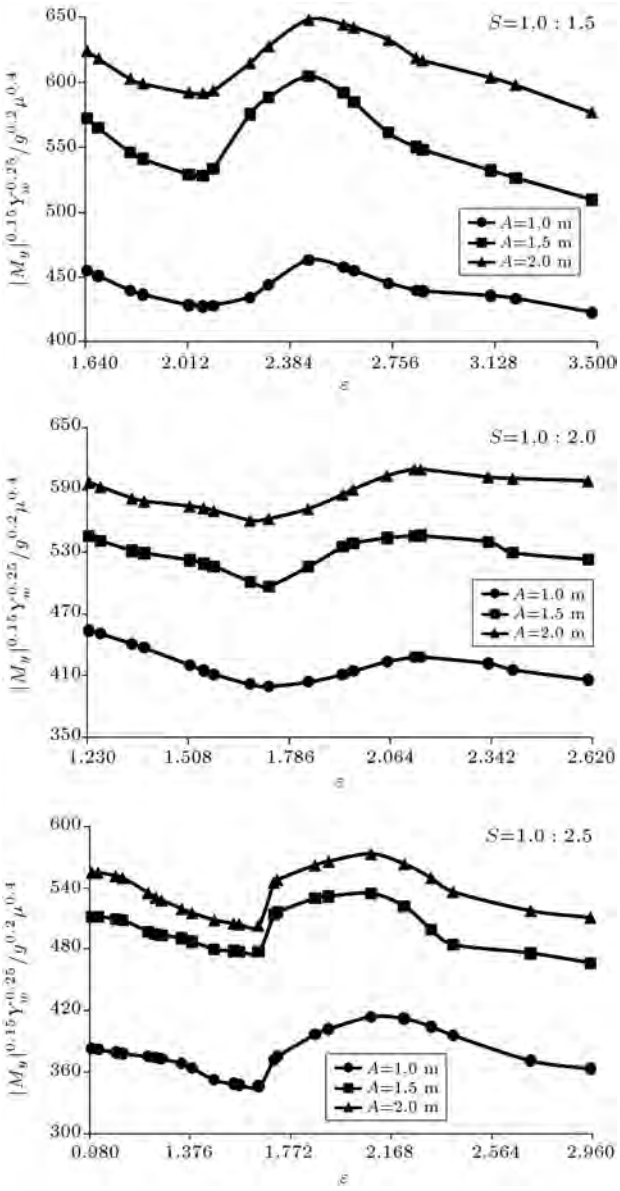

Figure 9. Variation of maximum moment for location L2 versus wave parameters.

wave breaking type cannot exactly clarify the observed trend.

Variations of F_R and $|M_y|$ with wave parameters for L1 (breakwater toe) are shown in Figure 11. As indicated in this figure, wave parameters are described by another dimensionless number, rather than ε. This means that the armor located in L1 has a different behavior compared with L2 and L4. In other words, for armors located far from the acting wave flow field, wave breaking has no role in the behavior of them. The best fit (linear), in this case, is found to be between $F_R T/\mu H^2$ and $\nu T/HD$, where μ and ν are the dynamic and kinematic viscosity of water, respectively.

Figure 12 demonstrates the relations among F_R, M_y, and wave parameters for L3 (maximum wave run-up level). It should be noted that the dimensionless numbers for L3 are the same as those of L1. This reveals that these two armor locations have analogous performances, since they are situated far enough from the main flow field of wave breaking.

3.3. Uplift instability mode

The uplift instability mode is quantified by the number U.I.N. (Eq. (13)). The armor weight acts as the stabilization force, while the wave force may work as either a stabilizing or destabilizing force, regarding its direction.

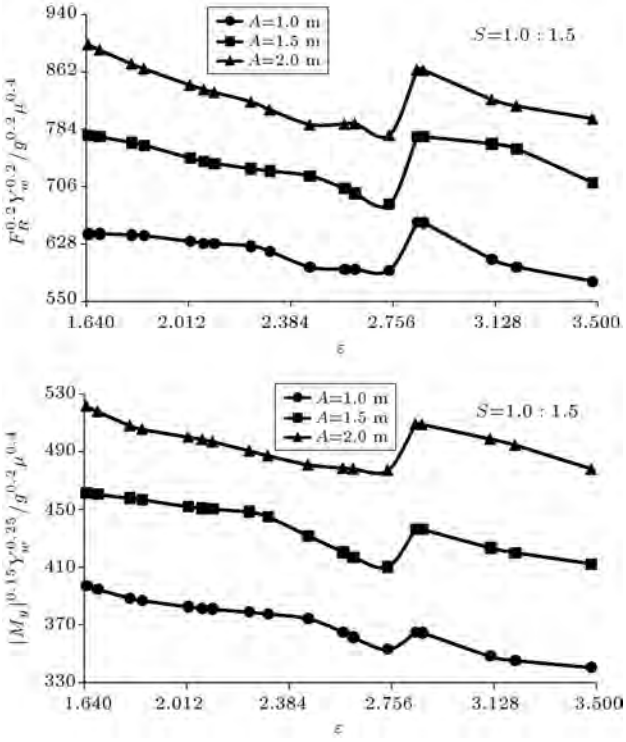

Figure 10. Variation of maximum force and moment for location L4 versus wave parameters.

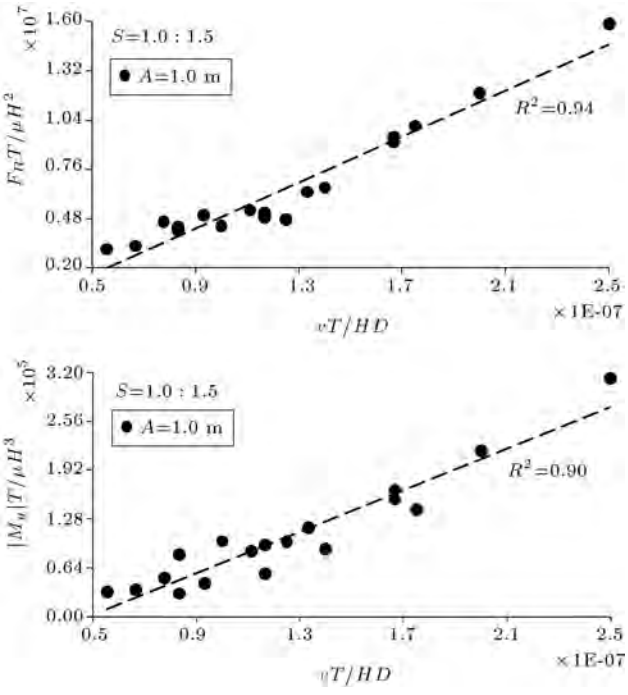

Figure 11. Variation of maximum force for location L1 versus wave parameters.

Variation of U.I.N. versus ε for location L2 and different slopes is presented in Figure 13. This figure indicates the effect of wave breaking type, and, also, the influence of armor diameter on the uplift stability. It is found that in all slopes, there exists a small

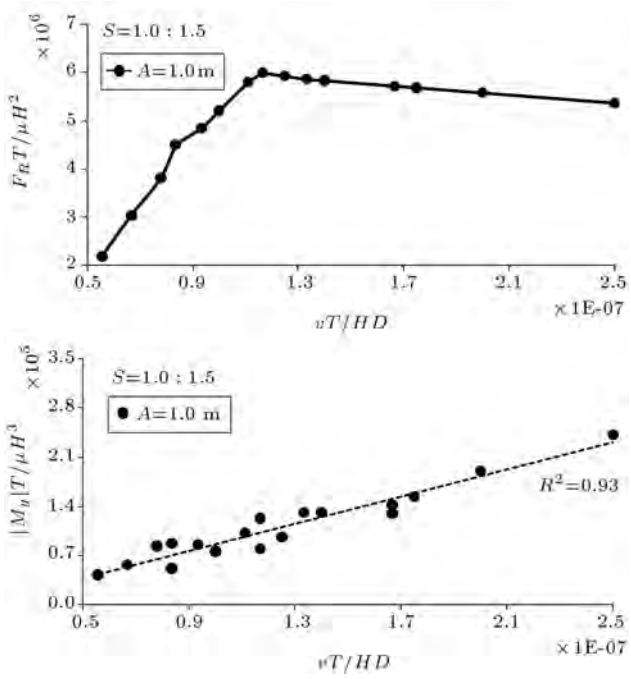

Figure 12. Variation of maximum force and moment for L3 versus wave parameters.

range of ε, in which $A = 2$ m has more critical uplift instability than $A = 1.5$ m. In these situations, by increasing the armor diameter, the unit experiences higher wave loads. However, the increased weight cannot compensate for the increased value of the wave loads, leading to less stability.

Variation of U.I.N values for L4 versus wave parameters is shown in Figure 14. This figure shows that for all armor dimensions, this location has the instability number of U.I.N > 1, and any increase in armor size will always lead to more stability.

Variation of U.I.N with wave parameters for L1 and L3 locations are shown in Figure 15. As indicated in this figure, in order to obtain a linear relation, wave parameters are described by another dimensionless number, rather than ε.

As a general comparison among armor locations from the view point of U.I.N (for parameters of $S = 1 : 1.5, D = 10, 15$ m and $A = 1.0$ m), Figure 16 shows that, in most cases, and also for their summation, armors located in L2, L4, L1 and L3 have a higher possibility of uplift instability, respectively. However, for $S = 1 : 1.5, D = 10, 15$ m and $A = 1.5, 2$ m, location L4 is more critical than L2. It is noted that all the above configurations are not mentioned in the figure, because of similarity.

3.4. Sliding instability mode

The sliding instability mode is enumerated by the number |S.I.N.| (Eq. (14)). In this mode, a combination of wave load, armor weight and friction force between the armor and the breakwater face

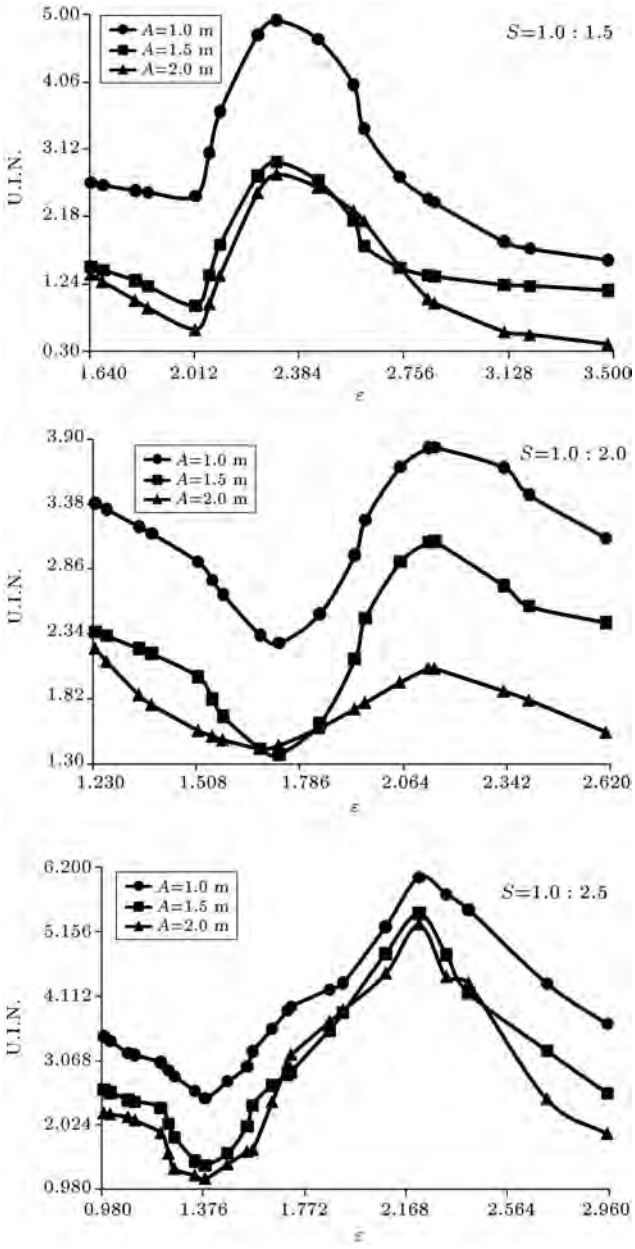

Figure 13. Variation of U.I.N. for location L2 versus wave parameters.

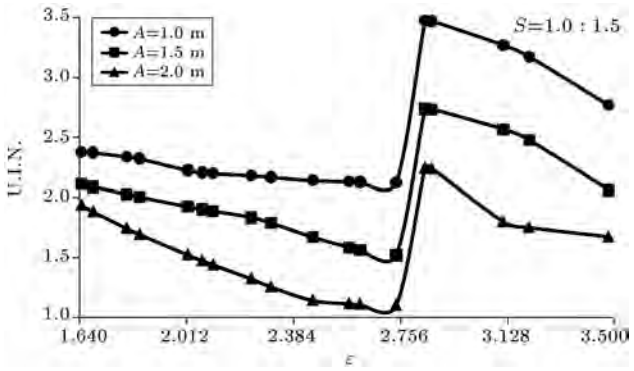

Figure 14. Variation of U.I.N. for location L4 versus wave parameters.

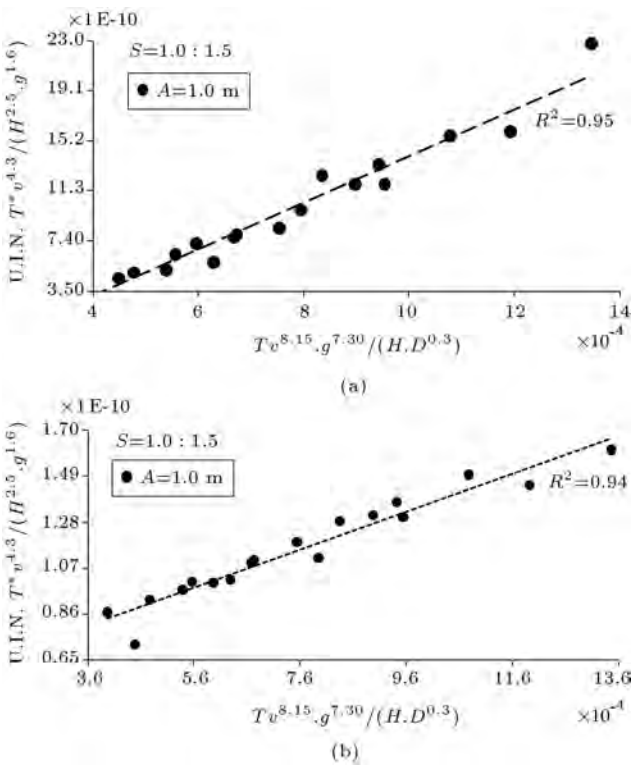

Figure 15. Variation of U.I.N. for L1 (a) and L3 (b) versus wave parameters.

is considered. The armor weight acts both as the stabilizing (movement towards the crest) or the destabilizing (movement towards the toe of the breakwater) force.

Variation of |S.I.N.| versus ε for location L2 and different slopes is presented in Figure 17. This figure points out the effect of wave breaking type and, also, the recital of the armor diameter. It is found that in all slopes, there are some ranges of ε where the raise in armor diameter leads to more instability. This happens because the increased friction force is not able to overcome the increased wave loads on the armor.

Variation of |S.I.N.| for location L4 versus wave parameters can be seen in Figure 18. This figure shows that by increasing the armor weight, in most cases, the sliding stability will increase, but there are some exceptions, as explained in the previous section. Values of |S.I.N.| for armors located in L1 and L3 are illustrated in Figure 19.

A general comparison of armor locations from the view point of |S.I.N.| for all wave parameters reveals that armors located in L2, L4, L3 and L1 have a higher possibility of sliding instability, respectively. This declaration is explained in Figure 20.

3.5. Overturning instability mode

The overturning instability mode is explained through the number |O.I.N.| (Eq. (17)). The armor weight,

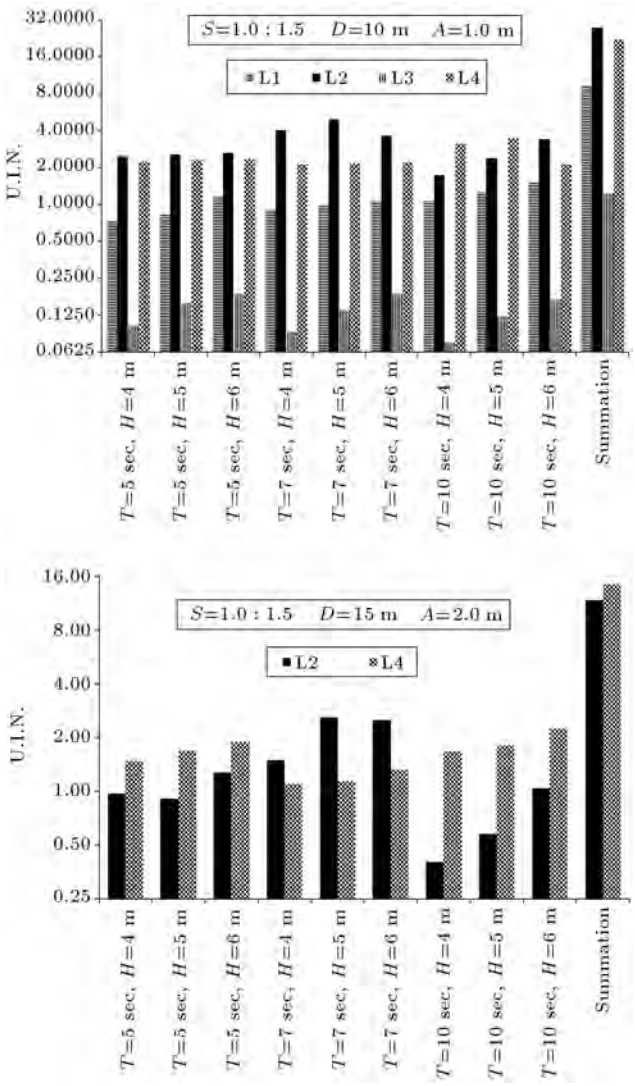

Figure 16. Comparison of uplift instability for different armor locations and wave parameters.

wave loads and moments take part in this number, which can be considered either stabilizing or destabilizing, making this instability mode the most complex one.

The relation of |O.I.N.| versus ε for location L2 and different slopes is illustrated in Figure 21. It is concluded that in all three slopes, by increasing the armor diameter, more overturning stability is achieved.

Variation of |O.I.N.| values for location L4 versus wave parameters can be observed in Figure 22. This figure shows that by increasing the armor weight, in all cases, the overturning stability will increase.

The |O.I.N.| magnitudes for armors located in L1 and L3 are shown in Figure 23.

A comparison of armor locations based on |O.I.N.| values for all wave parameters, is shown in Figure 24, which indicates that armors located in L2, L4, L1 and L3 have a higher possibility of overturning instability, respectively.

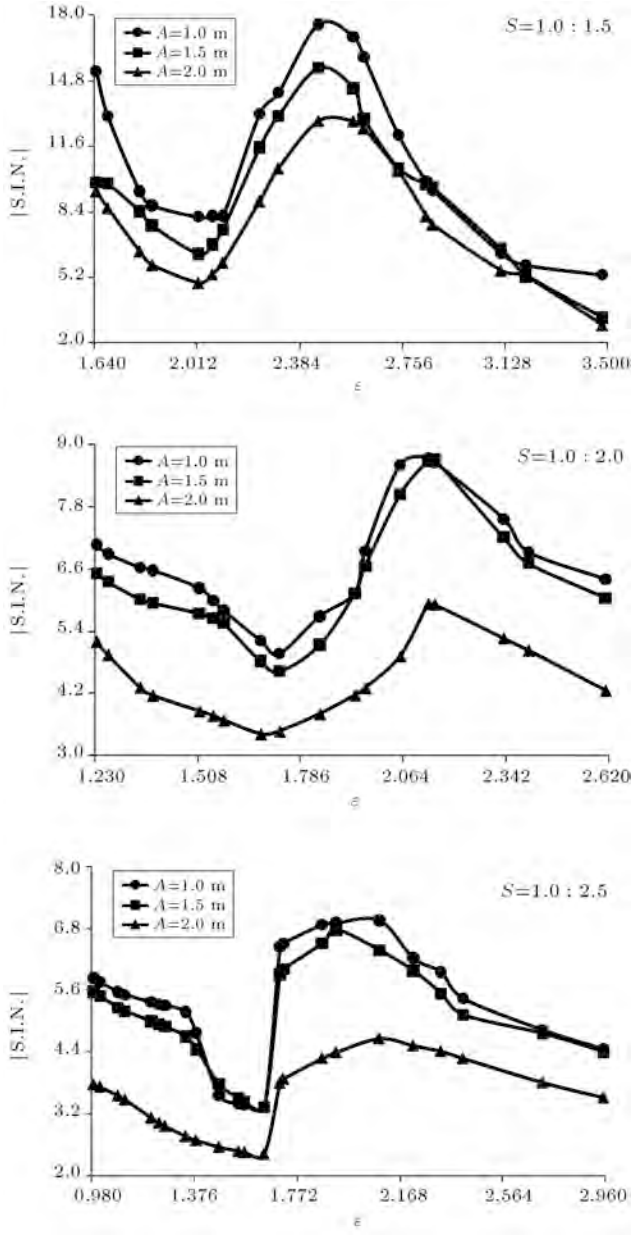

Figure 17. Variation of |S.I.N.| for location L2 versus wave parameters.

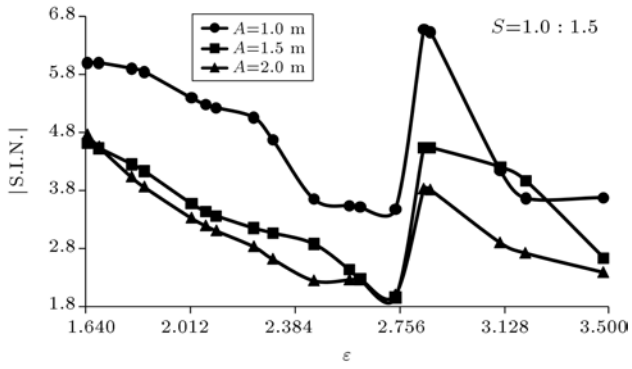

Figure 18. Variation of |S.I.N.| for location L4 versus wave parameters.

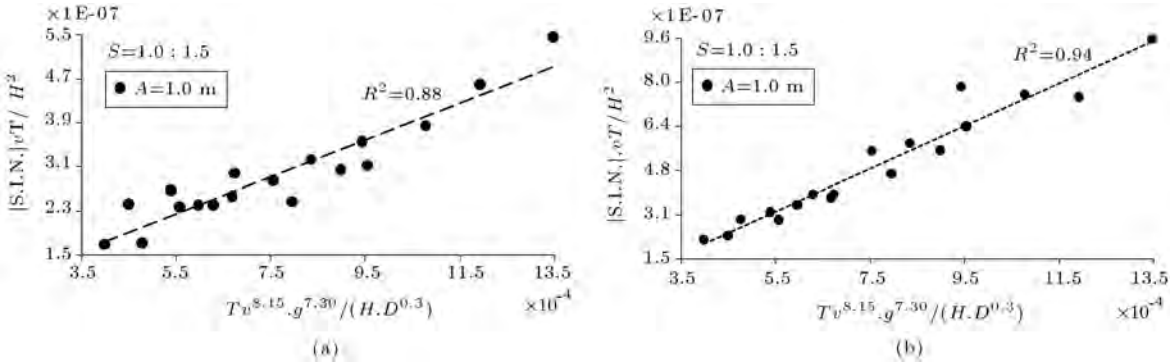

Figure 19. Variation of |S.I.N.| for L1 (a) and L3 (b) versus wave parameters.

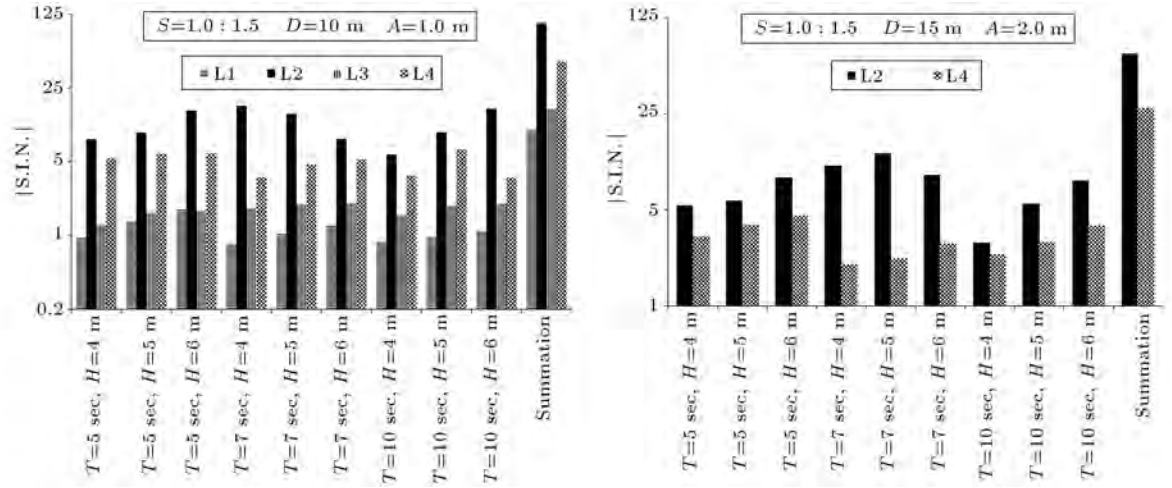

Figure 20. Comparison of sliding instability for different armor locations and wave parameters.

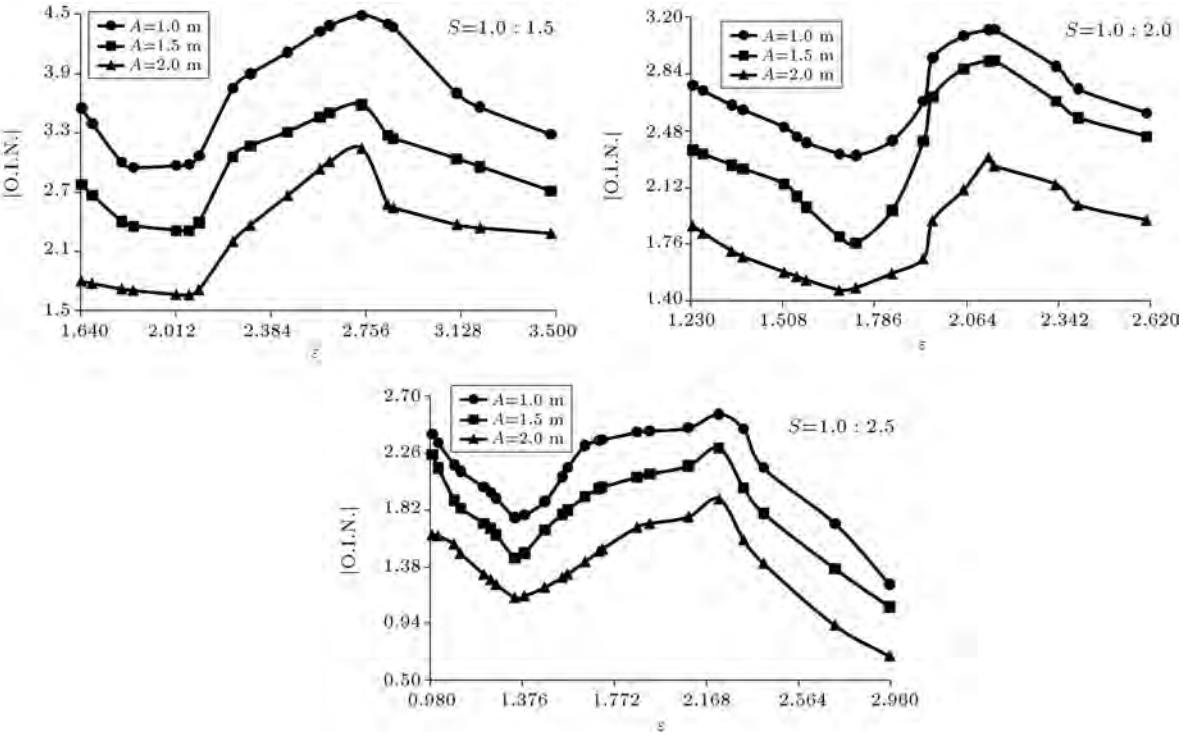

Figure 21. Variation of |O.I.N.| for location L2 versus wave parameters.

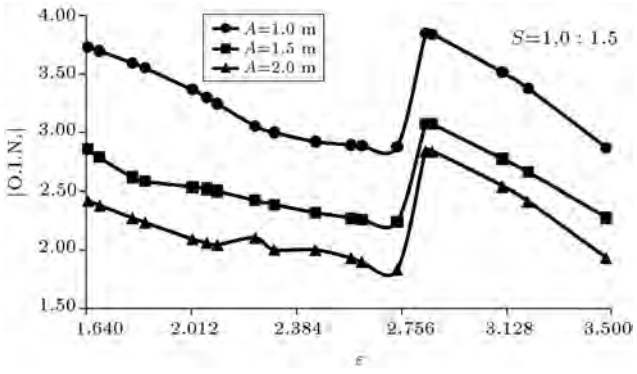

Figure 22. Variation of |O.I.N.| for location L4 versus wave parameters.

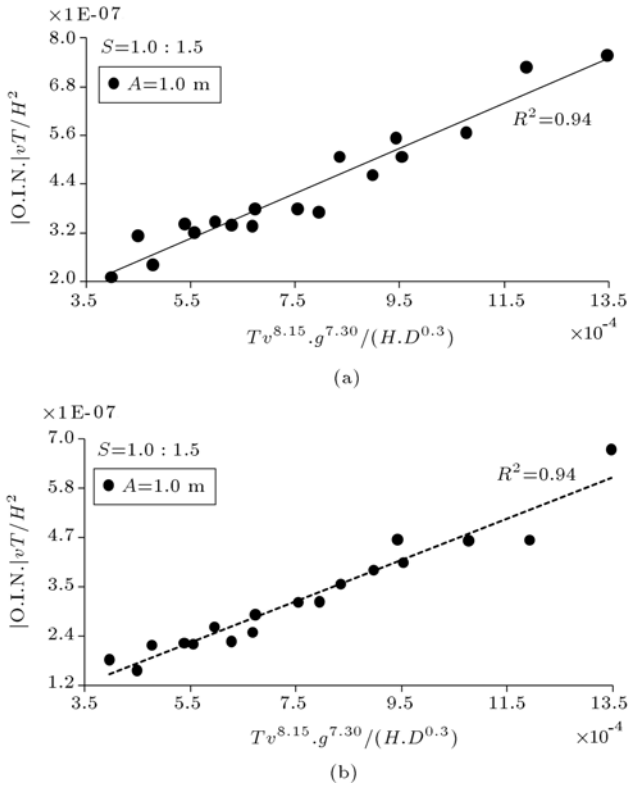

Figure 23. Variation of |O.I.N.| for L1 (a) and L3 (b) versus wave parameters.

4. Conclusions

In this paper, a novel force-based approach is proposed to study the stability of individual armor units in high-crested breakwaters. The applied forces and moments due to regular waves were computed for different armor locations and different wave characteristics. The proposed approach sheds some light on the mechanism of armor's stability. Instability numbers were introduced and calculated for analyzing the stability conditions of the units. The important results are summarized below:

- Design of the breakwater armor layer, based upon the wave-induced forces, can be a logical approach, substituting the conventional design procedure, which only uses wave height and does not offer in-depth physical reasoning for instability.
- Despite common expectation, higher waves do not necessarily require heavier armor units in breakwaters. In fact, what is more dominant in the design is the wave breaking mechanism. For the collapsing breaking type, higher waves require lighter armor units.
- Based on this study, for determining the armor unit weight, the breaking type (plunging, collapsing, surging), along with wave parameters, should be considered. The Iribarren number is proven to be an excellent parameter that contains basic wave characteristics and can be used for design purposes.
- The study showed that the critical locations for the instability of armor units are S.W.L. (still water

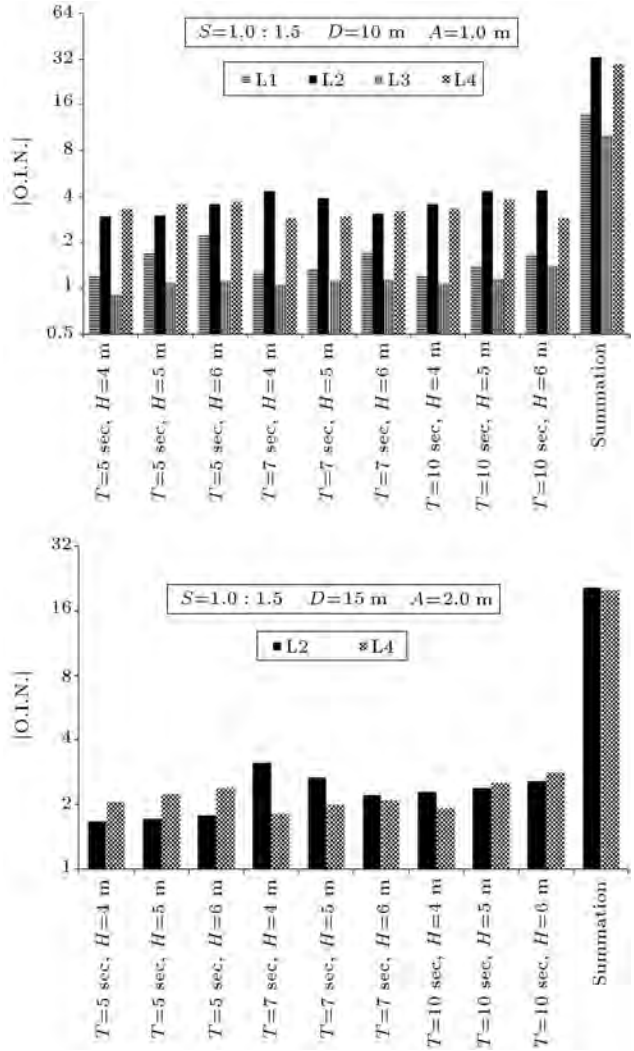

Figure 24. Comparison of overturning instability for different armor locations and wave parameters.

level) and Wave Run-Down (W.R.D.) elevations. So, rubble mound breakwaters are prone to damage due to wave attacks in the zone between S.W.L. and W.R.D. elevations.

- The proposed instability numbers can quantify and compare the effects of wave parameters on the armor units. Hence, the instability numbers can be used in the process of armor layer design based on the applied forces and moments.
- Sliding, overturning, and uplift are the most critical failure modes, respectively, in the majority of cases.

Variations in instability number (i.e. uplift, sliding and overturning), with respect to wave height, are not monotonic and are dominated by wave breaking mechanisms. Current research has produced preliminary results of the proposed geomechanical approach to designing breakwater armor units. A rigorous analysis of the stability of interlocked armor units, and examining blocks with different shapes, require further investigation.

Acknowledgments

The authors are grateful to the Parallel Processing Center of the Civil Engineering Department at Sharif University of Technology for providing computer facilities.

References

1. Novak, P., Moffat, A.I.B., Nalluri, C. and Narayanan, R., *Hydraulic Structures*, 4th Ed., pp. 575-670, Taylor and Francis, London, U.K. (2007).
2. Hudson, R.Y. "Laboratory investigations of rubble mound breakwaters", *Journal of Waterways, Harbors and Diversions*, **85**(3), pp. 93-121 (1959).
3. van der Meer, J.W., *Rubble mounds-recent modifications*, *Handbook of Coastal Engineering*, **1**, pp. 883-894, Gulf Publishing, U.S.A. (1990).
4. van der Meer, J.W., Kortenhaus, A., Bruce, T. and Franco, L. "Wave run-up and wave overtopping at armored rubble stones and mound", *Handbook of Coastal and Ocean Engineering*, World Scientific, Singapore, pp. 383-409 (2010).
5. Sigurdsson, G. "Wave forces on breakwater capstones", *Journal of Waterways and Harbors Division, ASCE*, **88**(3), pp. 27- 59 (1962).
6. Apelt, C.J. and Piorewicz, J. "Laboratory studies of breaking wave forces acting on vertical cylinders in shallow water", *Journal of Coastal Engineering*, **11**(3), pp. 263- 282 (1987).
7. Mizutani, N., Iwata, K., Rufin, T.M. and Kurata, K. "Laboratory investigation on the stability of a spherical armor unit of a submerged breakwater", *Proceeding of the 25th International Association for Hydraulic Research*, **4**, pp. 1400-1413 (1993).
8. Oumeraci, H. Klammer, P. and Partenscky, H.W. "Classification of breaking wave loads on vertical structures", *Journal of Waterway, Port, Coastal and Ocean Engineering*, **119**(4), pp. 381-397 (1993).
9. Pramono, W.T. "Wave Forces on cubical armor units on submerged and low-crested breakwaters", Ph.D. Thesis, University of Windsor (1997).
10. Mader, C.L., *Numerical Modeling of Water Waves*, 2nd Ed., CRC Press, U.S.A. (2005).
11. Sawaragi, T., *Coastal Engineering - Waves, Beaches, Wave-Structure Interactions*, Elsevier, Japan (1995).
12. Lara, J.L., Losada, I.J. and Guanche, R. "Wave interaction with low-mound breakwaters using a RANS model", *Journal of Ocean Engineering*, **35**(13), pp. 1388-1400 (2008).
13. Lo, E.Y.M. and Shao, S. "Simulation of near-shore solitary wave mechanics by incompressible SPH, LES and RANS methods", *Journal of Applied Ocean Research*, **24**, pp. 275-286 (2002).
14. Hsu, T.W., Lai, J.W. and Lan, Y.J. "Experimental and numerical studies on wave propagation over coarse grained sloping beach", *Proceedings of the 32nd International Conference on Coastal Engineering*, Shanghai, China (2010).
15. Hur, D.S. and Mizutani, N. "Numerical estimation of the wave force acting on a body on submerged breakwaters", *Journal of Coastal Engineering*, **47**(5), pp. 329-345 (2003).
16. Guanche, R., Losada, I.J. and Lara J.L. "Numerical analysis of wave loads for coastal structure stability", *Journal of Coastal Engineering*, **56**(5), pp. 543-558 (2009).
17. Pak, A. and Sarfaraz, M. "Numerical analysis of the stability of breakwater armor units due to sea wave attacks", *10th International Conference on Coasts, Ports and Marine Structures*, (ICOPMAS), Tehran, Iran (2012).
18. Minin, I.V. and Minin, O.V., *Computational Fluid Dynamics Technologies and Applications*, Janeza Trdine, Croatia (2011).
19. Garnier, E., Adams, N. and Sagaut, P. *Large Eddy Simulation for Compressible Flows*, Springer (2009).
20. Rodi, W., *Turbulence Models and Their Application in Hydraulics*, 3rd Ed., IAHR Monograph, Balkema, Rotterdam, The Netherlands (1993).
21. U.S. Army Corps of Engineers, *Coastal Engineering Manual*, Engineer Manual 1110-2- 1100, U.S. Army Corps of Engineers, Washington, U.S.A. (2006).
22. Paidousis, P.M., *Fluid-Structure Interactions*, Academic Press, U.S.A. (1998).
23. FlowScience. "FLOW-3D user's manual version 9.3", Santa Fe, New Mexico (2008).

24. B.S. "Falsework performance requirements and general design", Code 12812, British Standards (2004).
25. Sturm, T.W., *Open Channel Hydraulics*, McGraw-Hill, U.S.A. (2001).

Biographies

Ali Pak received his BS degree in Civil Engineering, in 1984, his MS degree in Soil Mechanics and Foundations, in 1989, and his PhD degree in Geotechnical Engineering, in 1997. He is currently Professor in the Department of Civil Engineering at Sharif University of Technology, Tehran, Iran. His main research focus is numerical modeling of soil/rock behavior under static and seismic loadings. He has more than 100 journal and conference papers in various fields including: liquefaction, soil improvement, environmental geotechnics, and petroleum geomechanics.

Mohammad Sarfaraz obtained a BS degree in Civil Engineering from the Power and Water University of Technology, Iran, in 2010, and an MS degree in Geotechnical Engineering from Sharif University of Technology, Tehran, Iran, in 2012. He ranked first among all students both in BS and MS degree programs. His main research interests include: wave-structure interaction, coastal and offshore structures, geotechnical earthquake engineering, lattice Boltzmann method, and impulsive water waves generated by landslides.